Yeast
Yeast 2004; **21**: 557–568.
Published online in Wiley InterScience (www.interscience.wiley.com). **DOI:** 10.1002/yea.1125

Research Article

Candida glabrata Ste20 is involved in maintaining cell wall integrity and adaptation to hypertonic stress, and is required for wild-type levels of virulence

Ana-Maria Calcagno[1,2], Elaine Bignell[1], Thomas R. Rogers[1], Mariana Canedo[1], Fritz A. Mühlschlegel[3] and Ken Haynes[1]*

[1]*Department of Infectious Diseases, Imperial College London, Du Cane Road, London W12 ONN, UK*
[2]*Center of Microbiology and Cell Biology, Venezuelan Institute for Scientific Research (IVIC), PO Box 21827, Caracas 1020A, Venezuela*
[3]*Research School of Biosciences, University of Kent at Canterbury, Kent CT2 7NJ, UK*

**Correspondence to:*
Ken Haynes, Department of Infectious Diseases, Imperial College London, Du Cane Road, London W12 ONN, UK.
E-mail: k.haynes@imperial.ac.uk

Received: 21 November 2003
Accepted: 25 February 2004

Abstract

The conserved family of fungal Ste20 p21-activated serine-threonine protein kinases regulate several signalling cascades. In *Saccharomyces cerevisiae* Ste20 is involved in pheromone signalling, invasive growth, the hypertonic stress response, cell wall integrity and binds Cdc42, a Rho-like small GTP-binding protein required for polarized morphogenesis. We have cloned the *STE20* homologue from the fungal pathogen *Candida glabrata* and have shown that it is present in a single copy in the genome. Translation of the nucleotide sequence predicts that *C. glabrata* Ste20 contains a highly conserved p21-activated serine–threonine protein kinase domain, a binding site for G-protein β subunits and a regulatory Rho-binding domain that enables the kinase to interact with Cdc42 and/or Rho-like small GTPases. *C. glabrata* Ste20 has 53% identity and 58% predicted amino acid similarity to *S. cerevisiae* Ste20 and can complement both the nitrogen starvation-induced filamentation and mating defects of *S. cerevisiae ste20* mutants. Analysis of *ste20* null and disrupted strains suggest that in *C. glabrata* Ste20 is required for a fully functional hypertonic stress response and intact cell wall integrity pathway. *C. glabrata* Ste20 is not required for nitrogen starvation-induced filamentation. Survival analysis revealed that *C. glabrata ste20* mutants, while still able to cause disease, are mildly attenuated for virulence compared to reconstituted *STE20* cells.

Keywords: ***Candida glabrata*; *STE20*; cell wall integrity; hypertonic stress response; virulence**

Introduction

The incidence of infections with *Candida* species has increased in the last 30 years and, just as dramatically, the proportion of infections caused by species other than *Candida albicans* has increased such that *Candida glabrata* now accounts for up to 20% of the cases of systematic candidiasis (Diekema *et al*., 2002). *C. glabrata* is able to induce disease in hosts whose systemic or local immune status is damaged, deteriorating or innately dysfunctional (Bodey *et al*., 2002). A major obstacle to effective management of *C. glabrata* infections is its increased resistance to azole antifungal therapy (Pfaller *et al*., 1999). Furthermore, *C. glabrata* infection is also associated with a high mortality (Gumbo *et al*., 1999). It is possible that an increased understanding of the biology that determines C. *glabrata* pathogenicity may aid in the development of novel strategies to effectively manage this increasingly important clinical problem.

Saccharomyces cerevisiae cells can respond to various environmental signals by activating a signal transduction pathway involving a transmembrane receptor G-protein complex linked to a

mitogen-activated protein kinase module (Leberer *et al*., 1992). The Ste20 protein kinase, a member of the p21-activated kinase (PAK) family, acts in the linkage between the G protein and the MAP kinase module. Ste20 is characterized by the presence of a conserved serine–threonine kinase domain near its C terminus, a binding site for G-protein ß-subunits in the non-catalytic carboxy-terminal region (Leeuw *et al*., 1998) and a regulatory PBD or CRIB domain at the N terminus that enables the kinase to interact with various signalling molecules and regulatory proteins of the cytoskeleton (Wu *et al*., 1996). *S. cerevisiae* Ste20 plays a role in pseudohyphal development and invasive growth (Leberer *et al*., 1997), is required for efficient activity of the pheromone response pathway (Ash *et al*., 2003) and an effective Hog1 mediated hypertonic stress response (Raitt *et al*., 2000). It also appears to play a role in the activation of myosin, adhesion of mating partners and vegetative functions relating to budding (Wu *et al*., 1997; Goehring *et al*., 2003).

Homologues of *S. cerevisiae STE20* have been described in a number of other fungal species. These include *C. albicans CST20* (*Candida*DB (**http://genolist.pasteur.fr/CandidaDB**; Accession No. Q92212; Kohler and Fink, 1996); *Cryptococcus neoformans STE20* (AF542531.1; Lengeler *et al*., 2000b; Wang *et al*., 2002); *Ustilago maydis* (AF299352.1; Weinzierl *et al*., 2002); and *Pneumocystis carinii* (AF332388; Kottom *et al*., 2003). These Ste20 proteins play important roles in mediating the regulation of various aspects of morphogenesis, conjugation, mating and pathogenicity.

We describe the cloning of the *C. glabrata STE20* homologue. We have constructed two different *Ste20* mutants that demonstrate that *C. glabrata* Ste20 is involved in maintaining cell wall integrity and the hypertonic stress response but is not required for nitrogen starvation-induced filamentation. Finally we demonstrate that *C. glabrata ste20* mutants, while still able to cause disease, are mildly attenuated compared to reconstituted *STE20* cells in a murine model of candidiasis.

Materials and methods

Strains and growth media

All the strains used in this study are listed in Table 1. Fungal cells were routinely cultured in YAPD (2% w/v peptone, 2% w/v glucose, 1% w/v yeast extract, 0.01% w/v adenine) or SC [0.17% w/v yeast nitrogen base without amino acids (Difco, Detroit, MI, USA), 2% w/v glucose and appropriate drop- out mix (Clontech, Basingstoke)] at 30 °C or 37 °C. For solid media 2% w/v agar was added prior to autoclaving. Synthetic low-ammonia dextrose (SLAD) media containing 10 μM ammonium sulphate as sole nitrogen source was prepared as previously described (Csank and Haynes, 2000). Other additives were filter-sterilized and added at the appropriate concentration to media after autoclaving.

Escherichia coli XL1-blue (Stratagene, La Jolla, CA) was used as the host strain for plasmid propagation.

Cloning of *C. glabrata STE20*

Degenerate primers (FD-20 and RD-20) were designed against alignments of the conserved p21-activated kinase domain of the Ste20 proteins from *S. cerevisiae, C. albicans and Cr. neoformans.* All primers used in this study are listed in Table 2. All PCR reactions were performed on a PCR-Engine (MJ Research, Watertown, MA) in 1 × PCR buffer (MBI, Vilnius, Lithuania) containing 1 U Taq polymerase and 100 ng *C. glabrata* ATCC 2001 genomic DNA. PCR conditions were 2 min at 94 °C, then 25 cycles of 60 s at 94 °C, 60 s at 45 °C and 2 min at 72 °C, followed by a final extension step of 7 min at 72 °C. The resulting PCR products were cloned into pGEM T-Easy (Promega, Southampton) and sequenced. A 482 bp fragment showed significant sequence similarity to fungal *STE20* genes.

A *C. glabrata* ATCC 2001 genomic DNA library constructed in YEp24 was a kind gift from Dominique Sanglard (CHUV, Lausanne, Switzerland). The 482 bp *STE20* PCR product was labelled with ^{32}P, using Ready-to-Go beads (Amersham-Pharmacia, Chalfont), and used to probe replicate filters of this library. Two positive colonies were identified that both contained 1.9 kb inserts. Sequencing of one plasmid (pAMC22) revealed an insert of 1863 bp. All other *STE20* sequence was obtained from the *C. glabrata* sequencing project (**http://cbi.labri.fr/Genolevures/index.php**).

Table 1. Fungal strains used in this study

Strain	Genotype	Reference
C. glabrata ATCC 2001	Wild-type	ATCC[a]
C. glabrata ΔHT6	*his3::URA3 Δura3 Δtrp1*	(31)
C. glabrata AM7	*his3::URA3 Δura3 Δtrp1 ste20^{644}::TRP1* pCgACH-3 [*HIS3*]	This study
C. glabrata AM22	*his3::URA3 Δura3 Δtrp1 ste20::HIS3*	This study
C. glabrata AM24	*his3::URA3 Δura3 Δtrp1 ste20::HIS3* pCgACT-14 [*TRP1*]	This study
C. glabrata AM25	*his3::URA3 Δura3 Δtrp1 ste20::HIS3* pAMC85 [*STE20, TRP1*]	This study
S. cerevisiae L5366	*ura3/ura3*	FLC[b]
S. cerevisiae L5624	*ura3/ura3 ste20/ste20*	FLC[b]
S. cerevisiae AM10	*ura3/ura3* YEp24 [*URA3*]	This study
*S. cerevisiae*AM31	*ura3/ura3 ste20/ste20* YEp24 [*URA3*]	This study
S. cerevisiae AM32	*ura3/ura3 ste20/ste20* pAMC86 [*CgSTE20 URA3*][c]	This study
S. cerevisiae Y00956	*MAT***a** *his3 leu2 met15 ura3 ste20::kanMx4*	EUROSCARF[d]
S. cerevisiae AM33	*MAT***a** *his3 leu2 met15 ura3 ste20::kanMx4* YEp24 [*URA3*]	This study
S. cerevisiae AM34	*MAT***a** *his3 leu2 met15 ura3 ste20::kanMx4* pAMC86 [*CgSTE20 URA3*][c]	This study
S. cerevisiae Y10956	*MATα his3 leu2 lys2 ura3 ste20::kanMx4*	EUROSCARF[d]
S. cerevisiae AM35	*MATα his3 leu2 lys2 ura3 ste20::kanMx4* YEp24 [*URA3*]	This study
S. cerevisiae AM36	*MATα his3 leu2 lys2 ura3 ste20::kanMx4* pAMC86 [*CgSTE20 URA3*][c]	This study

[a] American Type Culture Collection.
[b] Fink Laboratory Collection.
[c] *Cg* is prefixed to differentiate the *C. glabrata* gene from the *S. cerevisiae* gene.
[d] European *Saccharomyces cerevisiae* archives for functional analysis.

Table 2. Primers used in this study[a]

Primer	Primer sequence (5′ to 3′)	Description
FD-20	GTNAARATHGGNCARGGNGC	Degenerate *STE20* forward +1869 to +1889
RD-20	TCNGGNGCCATCCARTANGG	Degenerate *STE20* reverse +2351 to +2331
FDCSTE20-T	CTTCGTTGCCAAAGCTACCATC	*STE20* forward +1605 to +1627
RDCSTE20-T	TGAGCACAGAAACCAAAATCGG	*STE20* reverse +2266 to +2288
F1-STE20	GACGGATGTTTATTCTCGATGA	*STE20* forward −539 to −517
R1-STE20	CCTAAATCTCCAATCTAGTATG	*STE20* reverse −84 to −106
F2-STE20	CGAGTTCAGAGCGGTTTCCAGT	*STE20* forward +2862 to +2884
R2-STE20	TCGATGTCAGGCCAGTCCCTCTG	*STE20* reverse +3349 to +3326
F2exDC-STE20	ATGGAAGAGAAAGCAGGCATGGA	*STE20* forward −687 to −665
RIntHis	CGGGATCATCTCTGTGGATAGC	*HIS3* reverse +453 to +432

[a] Numbers relate to position with respect to start codon of appropriate *C. glabrata* ORF.

Disruption of *C. glabrata STE20*

Two different strategies were adopted to construct *C. glabrata* loss of function *ste20* mutants, i.e. gene disruption in the serine–threonine protein kinase catalytic domain and complete replacement of the open reading frame, resulting in a null allele.

A 681 bp *Eco*RI–*Eco*RI fragment from pAMC22, containing the entire putative p21-activated serine–threonine protein kinase catalytic domain was subcloned into the *Eco*RI site of pBluescriptIISK$^+$ to give the plasmid pAMC75.1. This was digested with *Tth*111I and the *C. glabrata TRP1* gene inserted resulting in disruption of

the *C. glabrata STE20* ORF at position +1933, and truncation at codon 644. The resulting clone (pAMC75.2) was used as template for PCR, with the primer pair FDCSTE20-T + RDCSTE20-T (Table 2), to generate a linear *STE20* gene disruption cassette. This cassette was used to transform *C. glabrata* ΔHT6. Tryptophan prototrophs were selected and *STE20* interruption was confirmed by PCR (data not shown). A representative strain was selected and transformed with pCgACH-3 (Kitada *et al.*, 1996) to give a prototrophic *ste20* disrupted strain. This strain was designated *C. glabrata* AM7 (*his3::URA3* Δ*ura3* Δ*trp1 ste*20^{644}*::TRP1* pCgACH-3).

Construction of a *C. glabrata ste20* null allele

To construct a *C. glabrata ste20* null allele, a 455 bp 5′ fragment (−539 to −84) and a 487 bp 3′ fragment (+2862 to +3349) were amplified by high fidelity PCR, using *C. glabrata* ATCC 2001 genomic DNA as a target, and the primer pairs F1-STE20 + R1-STE20 and F2-STE20 + R2-STE20, respectively (Figure 1A). The *STE20* stop codon is at +2748. The 455 bp fragment was cloned into the *Sma*I site of pBluescriptSKII$^+$ to give the plasmid pAMC93. This plasmid was digested with *Eco*RI, blunt-ended and *C. glabrata HIS3* ligated in to give pAMC94. This plasmid was digested with *Hin*dIII, blunt-ended and

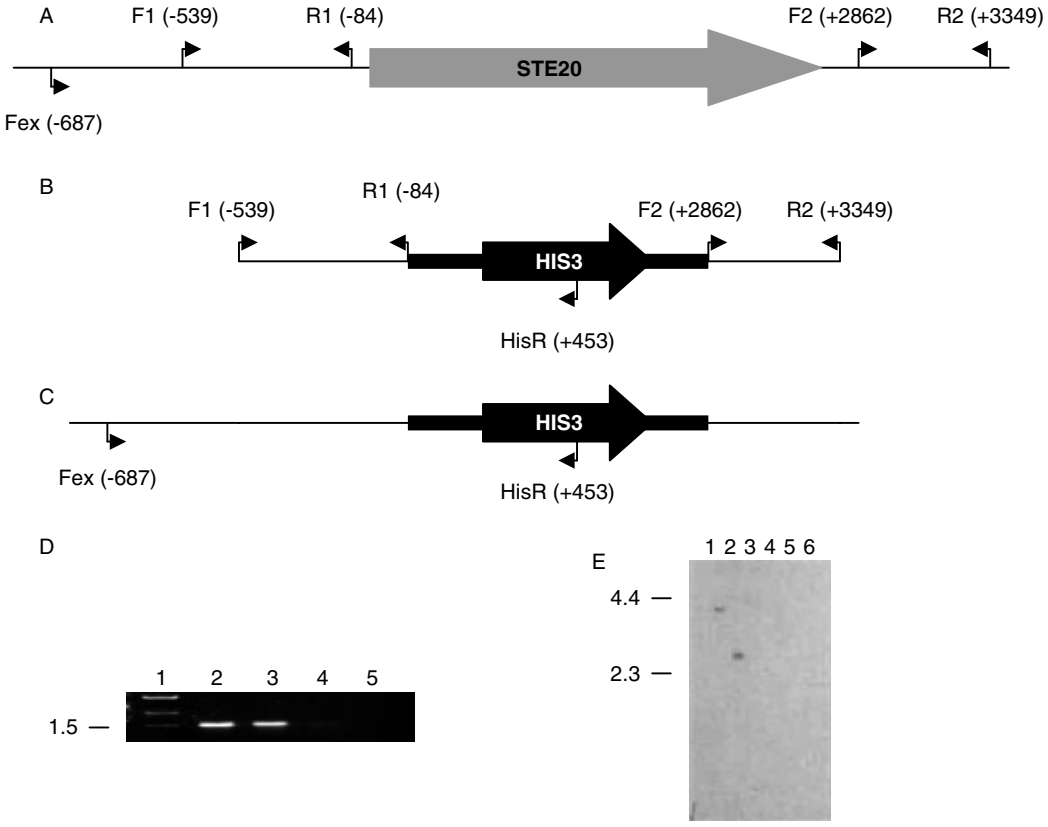

Figure 1. Construction of a *C. glabrata ste20* null allele. (A**)** *C. glabrata STE20* genomic locus showing relative positions of primers used for construction of the *ste20* disruption cassette: F1 (F1−STE20), R1 (R1−STE20), F2 (F2−STE20), R2 (R2−STE20) and confirmation of integration Fex (FexDCSTE20). Not to scale. (B**)** *STE20* disruption cassette showing position and orientation of the *HIS3* internal primer HisR (RIntHis). (C**)** *ste20* null allele genomic locus showing position of primers Fex and HisR used to confirm correct integration of the *ste20* disruption cassette. (D**)** PCR analysis of two *ste20* null mutants (2, 3), including AM22 (3) and ATCC 2001 (5) with primers Fex and HisR. Expected product size is 1.5 kb. Lane 4 was left empty and lane 1 contains 1 kb marker ladder. (E**)** Southern analysis of *C. glabrata* ATCC 2001 (1, 2), AM22 (3, 4) and another *ste20* mutant (5, 6), genomic DNA was digested with *Xba*I (1, 3, 5) or *Ava*I (2, 4, 6). The blot was probed with a *STE20* fragment (+1605/+2266) and confirms loss of the genomic *STE20* allele in *C. glabrata* AM22. Figures to the left of (D) and (E) represent size markers in kb

the 487 bp fragment was cloned in. The resulting plasmid (pAMC95) was used as template for PCR with F1-STE20 and R2-STE20 primers (Table 2), to generate a linear *STE20* gene replacement cassette (Figure 1B). This cassette was used to transform *C. glabrata* ΔHT6. Histidine prototrophs were selected. Homologous integration and gene replacement were confirmed by Southern analysis and PCR (Figure 1C-E), using the primers FexDC-STE20 (external to the disruption cassette) and RintHis (internal *HIS3*). A representative strain (AM22) was selected and transformed with pCgACT-14 (Kitada *et al*., 1996) to give a prototrophic *ste20* null strain. This strain was designated *C. glabrata* AM24 (*his3::URA3* Δ*ura3* Δ*trp1 ste20::HIS3* pCgACT-14).

Reconstitution of *C. glabrata STE20*

To reconstitute *C. glabrata STE20* in AM22, a 3887 bp fragment containing the entire *STE20* gene was obtained by high fidelity PCR from genomic DNA with the primers F1-STE20 and R2-STE20. Plasmid pAMC85 was constructed by cloning this fragment into *Sac*I-digested blunt-ended pCgACT-14. To reintroduce *STE20* into *C. glabrata* AM22, this strain was transformed with pAMC85. Tryptophan prototrophs were selected. Reconstitution of *STE20* was confirmed by PCR with the primer pair F1-STE20 + R1-STE20 (data not shown). A representative *STE20* reconstituted strain *C. glabrata* AM25 (*his3::URA3* Δ*ura3* Δ*trp1 ste20::HIS3* pAMC85 [*STE20, TRP1*]) was selected for further analysis.

Complementation of *S. cerevisiae ste20* mutants

The 3887 bp *C. glabrata STE20* fragment produced by PCR using the primers F1-STE20 and R2-STE20 was cloned into *Bam*HI-digested blunt-ended YEp24. The resultant plasmid pAMC86 was used to transform the diploid *S. cerevisiae ste20* mutant L5624 (*ura3/ura3 ste20/ste20*) (Mosch and Fink, 1997). Uracil prototrophs were selected and uptake of *C. glabrata STE20* was confirmed by PCR with the primer pair F1-STE20 + R1-STE20 (data not shown). A representative *S. cerevisiae* transformant AM32 (*ura3/ura3 ste20/ste20* pAMC86 [*CgSTE20 URA3*]) was selected. *S. cerevisiae* L5624 was also transformed with empty YEp24 to generate the strain AM31.

In addition, the haploid *S. cerevisiae ste20 MAT***a** mutant Y00956 (*MAT***a** *his3 leu2 met15 ura3 ste20::kanMx4*) was transformed with either YEp24 or pAMC86 to yield strains AM33 (*MAT***a** *his3 leu2 met15 ura3 ste20::kanMx4* YEp24 [*URA3*]) and AM34 (*MAT***a** *his3 leu2 met15 ura3 ste20::kanMx4* pAMC86 [*URA3 CgSTE20*]), respectively. Similarly, the *ste20 MAT*α mutant Y10956 (*MAT*α *his3 leu2 lys2 ura3 ste20::kanMx4*) was transformed with both plasmids to yield AM35 (*MAT*α *his3 leu2 lys2 ura3 ste20::kanMx4* YEp24 [*URA3*]) and AM36 (*MAT*α *his3 leu2 lys2 ura3 ste20::kanMx4* YEp24 [*URA3*]).

A prototrophic wild-type strain, designated AM10, was constructed by transforming *S. cerevisiae* L5366 (*ura3/ura3*) with YEp24.

Mating assays

To determine if the protein encoded by *C. glabrata STE20* could complement the mating defect of haploid *S. cerevisiae ste20* null mutants Y00956 and Y10956, their YEp24 transformants AM33 and AM35 plus the *C. glabrata STE20* complemented pair AM34 and AM36 were crossed to each other in a series of patch matings. After 48 h at 30 °C on YAPD portions of each patch were transferred to SC without lysine and methionine, then incubated for a further 48 h at 30 °C.

Model of systemic candidiasis

To determine the virulence characteristics of the *C. glabrata ste20* mutant AM24 in relation to the *STE20* reconstituted strain AM25 we used a murine model of systemic candidiasis that we have recently developed (Calcagno *et al*., 2003).

Briefly groups of 15 cyclophosphamide (200 mg/kg) immunosuppressed CD1 mice (25–28 g) were infected via the lateral tail vein with equivalent doses of the *C. glabrata STE20* reconstituted strain AM25 (6.2×10^7) or the *C. glabrata ste20* mutant AM24 (6.5×10^7). Mice were sacrificed when the predetermined end-point of 20% weight loss was reached. Survival curves were compared using Kaplan–Meier Log Rank analysis.

Results

C. glabrata STE20 encodes a member of the fungal Ste20 protein kinase family

PCR amplification with degenerate primers FD-20 and RD-20 yielded two amplicons of 680 bp and 482 bp, respectively. Sequencing of these two products revealed that the 482 bp band had substantial sequence similarity to a number of fungal *STE20* genes. Use of this PCR product to screen a *C. glabrata* genomic library in YEp24 yielded two independent clones, each apparently containing the same 1863 bp insert. Sequence analysis of one of these clones revealed that the insert contained sequence from a serine threonine protein kinase catalytic domain, a stop codon and putative polyadenylation signal sequence. The 5′ region was absent. This sequence showed significant similarity to the *S. cerevisiae STE20* gene. The remaining sequence was obtained from Bernard Dujon and Christophe Hennequin of the *C. glabrata* genome-sequencing project (**http://cbi.labri.fr/Genolevures/index.php**).

The completed sequence reveals a predicted uninterrupted open reading frame of 2748 bp, the putative TATA elements in the 5′ untranslated region are 25 and 45 bp upstream from the proposed initiation codon and a possible poly-A signal sequence is located at position +2798 to +2804. The translated sequence is predicted to encode a protein of 916 amino acids with a molecular weight of 100.3 kDa. The encoded protein has substantial amino acid sequence similarity to members of the Ste20 family of serine–threonine protein kinases, including those of *S. cerevisiae* (53%) (Ramer and Davis, 1993), *Sz. pombe* (48%) (Ottilie *et al.*, 1995), *P. carinii* (43%) (Kottom *et al.*, 2003), *Cr. neoformans* (42%) (Lengeler *et al.*, 2000b) and *C. albicans* (38%) (Leberer *et al.*, 1996). This sequence similarity is particularly striking in the highly conserved catalytic domain (Figure 2) typical of the serine–threonine protein kinase family (Hanks *et al.*, 1988). The *C. glabrata* putative catalytic domain has the conserved boundaries and 11 subdomains characteristic of the family (Hanks and Quinn, 1991). In addition the predicted sequence contains a binding site (NSSLSPLVK-LAR) for G-protein ß-subunits (Leberer *et al.*, 2000) between amino acids 877 and 889 (Figure 2). The N-terminus of the protein contains a putative non-catalytic regulatory motif (ISTPYNPKHIY-HVGVD) between amino acids 334 and 350 that is similar to the Cdc42 binding sites of mammalian $p65^{PAK}$ or $p120^{ACK}$ (Widmann *et al.*, 1999). This sequence binds Cdc42 or Rac (Burbelo *et al.*, 1995) and facilitates interactions between kinases and various signalling molecules and regulatory proteins of the cytoskeleton.

Two additional *STE20*-like protein kinase encoding genes have been described in *S. cerevisiae CLA4* and *SKM1* (Martin *et al.*, 1997). We have designated this ORF *C. glabrata STE20* for a number of reasons. BLASTP analysis of the predicted translation product reveals more similarity to *S. cerevisiae* Ste20 ($p = 9.2^{e-179}$) than to Cla4 ($p = 8.2^{e-86}$). There is an annotated *C. glabrata* protein (GAGL–CDS 0666.1; **http://cbi.labri.fr/Genolevures/C_glabrata-Genolevures-rc1.aa**) that shows much higher similarity to *S. cerevisiae* Cla4 ($p = 1.3^{-260}$) than to Ste20 ($p = 6.1^{e-97}$). Finally, and most convincingly, the protein encoded by *C. glabrata STE20* can complement the mating defect of *S. cerevisiae ste20* strains.

Southern analysis reveals that the *C. glabrata STE20* gene is present as a single copy in the genome (data not shown).

C. glabrata STE20 complements the mating and filamentation defects of *S. cerevisiae ste20 strains*

Mating of the *S. cerevisiae* strains AM34 and AM36, *ste20* mutants transformed with *C. glabrata STE20*, resulted in viable progeny (Figure 3). These data demonstrate that the product of the *C. glabrata STE20* gene can rescue the mating defect of *ste20* mutants (Kohler and Fink, 1996; Leberer *et al.*, 1992).

We were also able to show that the nitrogen starvation-induced filamentation defect of diploid *S. cerevisiae ste20/ste20* mutants was complemented by introduction of *C. glabrata STE20*. The extent of filamentation was gauged semi-quantitatively using the criteria developed by O'Rourke and Herskowitz (1998). The *S. cerevisiae ste20/ste20* diploid strain L5624 had 11% weakly-filamenting and 89% non-filamenting colonies ($n = 200$) when cultured on SLAD for 96 h at 30 °C compared to 100% ($n = 200$) of wild-type AM10 colonies with profuse filamentation (Figure 4). Transformation of *S. cerevisiae* L5624 with the

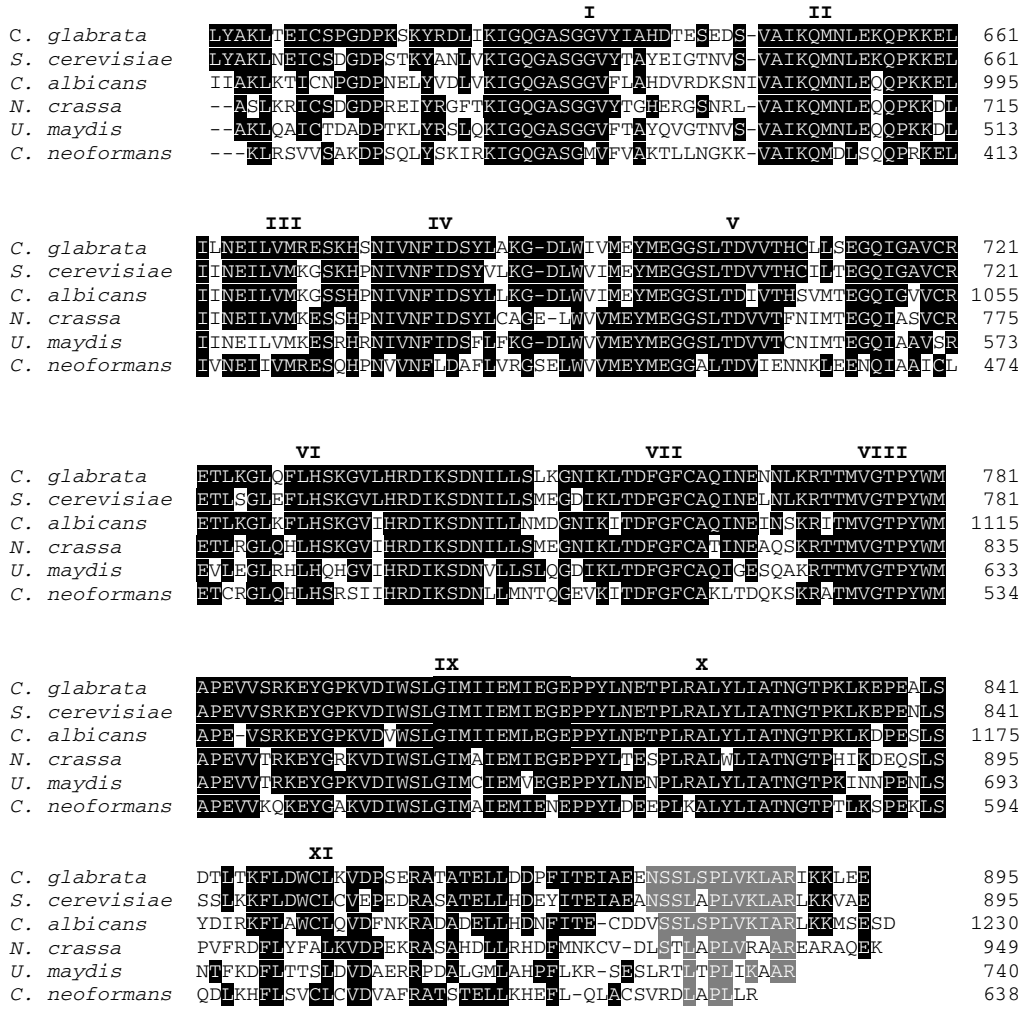

Figure 2. Alignment of the putative catalytic domain of *C. glabrata* Ste20 with Ste20 proteins from *S. cerevisiae, C. albicans, N. crassa, U. maydis* and *Cr. neoformans*. The Roman numerals above the amino acid sequence indicate the 11 subdomains characteristic of the protein kinase catalytic domain, while the arabic numerals to the sides of the sequence indicate relative amino acid numbers. The putative G-protein ß-subunit binding site is shown in grey

C. glabrata STE20-containing plasmid pAMC86 resulted in partial complementation of the nitrogen starvation-induced filamentation defect seen in this strain (Figure 4), as 59% of colonies had robust filamentation, 31% filamented weakly and only 10% exhibited no filamentation ($n = 200$). These data suggest that in addition to having sequence similarity to *S. cerevisiae STE20*, the *C. glabrata* gene encodes a functional homologue of Ste20.

C. glabrata STE20 is not required for nitrogen starvation-induced filamentation

We have demonstrated that *C. glabrata* produces pseudohyphae, similar to diploid *S. cerevisiae* strains, in response to nitrogen starvation and that the transcription factor Ste12 is required for this response (Csank and Haynes, 2000; Calcagno *et al*., 2003b). We therefore sought to determine if *C. glabrata* Ste20 is also required for nitrogen starvation-induced filamentation. The *ste20* null mutant AM24 and *ste*20^{644}-disrupted strain AM7 had no significant defects in filamentation on nitrogen starvation medium (data not shown). Their filamentation responses were equivalent to those of both *STE20* reconstituted and wild-type cells. These data suggest that *C. glabrata* Ste20 is not required for nitrogen starvation-induced filamentation.

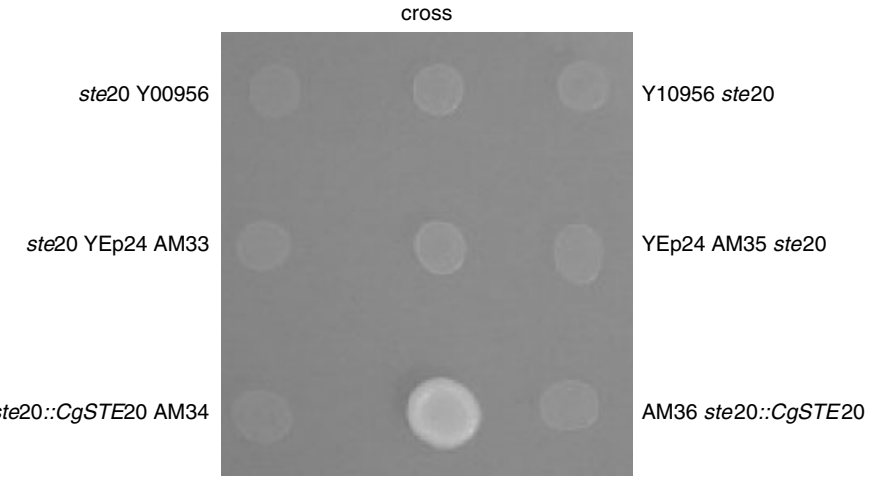

Figure 3. *C. glabrata STE20* complements the mating defects of *S. cerevisiae ste20* mutants. Haploid *S. cerevisiae* pairs Y00 956 (*MAT***a** *ste20*) and Y10 956 (*MATα ste20*), AM33 (*MAT***a** *ste20* YEp24) and AM35 (*MATα ste20* YEp24) plus AM34 (*MAT***a** *ste20 CgSTE20*) and AM36 (*MATα ste20 CgSTE20*) were patch mated. After 48 h culture on YPAD the patches were transferred to SC without methionine and lysine and cultured for a further 48 h at 30 °C. The left and right columns represent the parental strains as indicated and the centre column the products of mating

C. glabrata STE20 is involved in maintaining cell wall integrity and adaptation to hypertonic stress

To determine the role that *C. glabrata* Ste20 plays in adaptation to hypertonic stress and/or in maintaining cell wall integrity strains AM7 and AM24 were cultured in the presence of NaCl, sorbitol, calcofluor white and SDS. The *C. glabrata ste*20^{644} strain AM7 is unable to grow in the presence of 1 M NaCl at 30 °C, whereas the *ste20* null mutant AM24 has a moderate growth defect. Both phenotypes are much less pronounced at 37 °C. Both strains have a slight growth defect in the presence of 1.5 M sorbitol at 30 °C, that is completely rescued at 37 °C (Figure 5). Both strains have substantial growth defects on calcofluor white and are unable to grow on SDS at 30 °C. No growth defect was seen on calcofluor white at 37 °C but the SDS growth defect was still pronounced at this temperature. These data suggest that *C. glabrata* Ste20 is required for a fully functional hypertonic stress response and maintenance of an intact cell wall integrity pathway.

STE20 is required for wild-type levels of *C. glabrata* virulence

We have developed a model of murine candidiasis (Calcagno *et al.*, 2003) and used it to compare the virulence of *C. glabrata ste20* (AM24) cells and *STE20* (AM25) reconstituted cells. *C. glabrata ste20* cells were statistically significantly less able to cause disease than reconstituted *STE20* cells (Figure 6; $p = 0.011$, Kaplan–Meier log rank analysis). These data suggest that while still able to cause disease *ste20* mutants are mildly attenuated for virulence compared to *STE20* reconstituted strains.

Discussion

The *C. glabrata* protein Ste20 is a member of the highly conserved p21-activated serine–threonine protein kinase family. In fungi these proteins are involved in the regulation of multiple cellular processes including mating, filamentation, maintenance of cell wall integrity, adaptation to hypertonic stress, morphogenesis and virulence (Xu, 2000). In *S. cerevisiae* Ste20 is a component of three relatively well-defined signalling pathways that mediate mating, the hypertonic stress response and filamentous growth (Xu, 2000) and the less well-characterized *STE* vegetative growth pathway which functions to promote cell wall integrity (Cullen *et al.*, 2000; Lee and Elion, 1999). Components of these pathways have also been shown to play important roles in the pathogenesis of *Candida* species (Calcagno *et al.*, 2003; Lo *et al.*, 1997). We

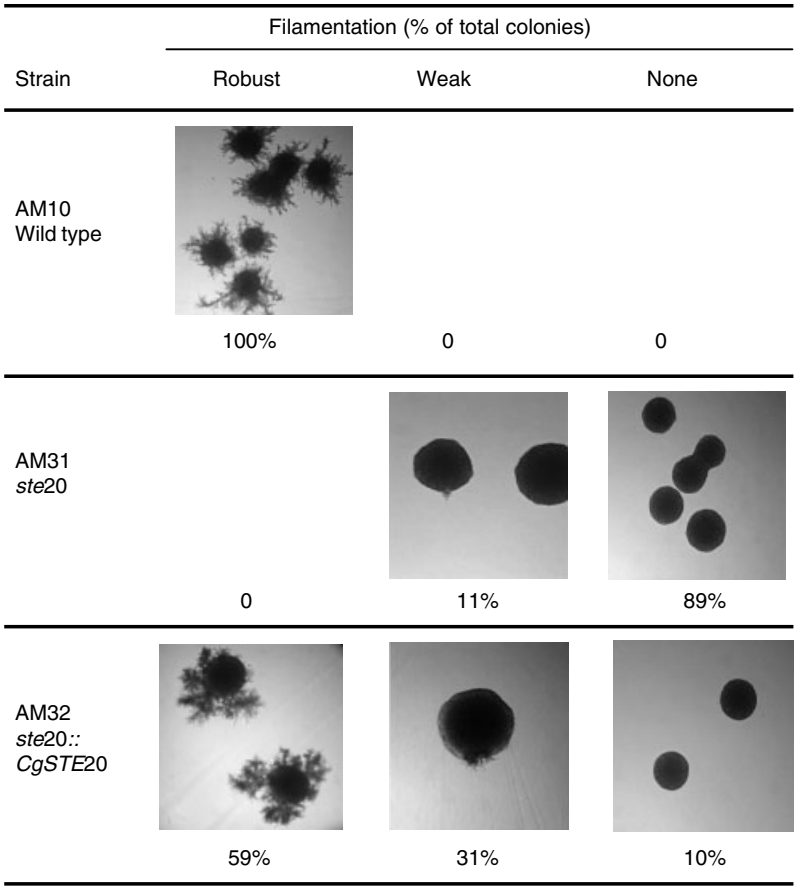

Figure 4. *C. glabrata* Ste20 partially complements the *S. cerevisiae ste20* nitrogen starvation-induced filamentation defect. Wild-type (AM10), *ste20* (AM31) and *STE20* reconstituted (AM32) *S. cerevisiae* strains were cultured on SLAD medium for 9 days at 30 °C. The resultant colonies were viewed with a Leitz Laborlux 12 microscope using a 10× objective. Images were captured with a Nikon CoolPix digital camera and imported into Microsoft Word. Two hundred colonies were counted for each strain and classified according to the scale of O'Rourke and Herskowitz (1998). Images show representative colonies from each classification. Figures indicate percentage of each strain within each filamentation class

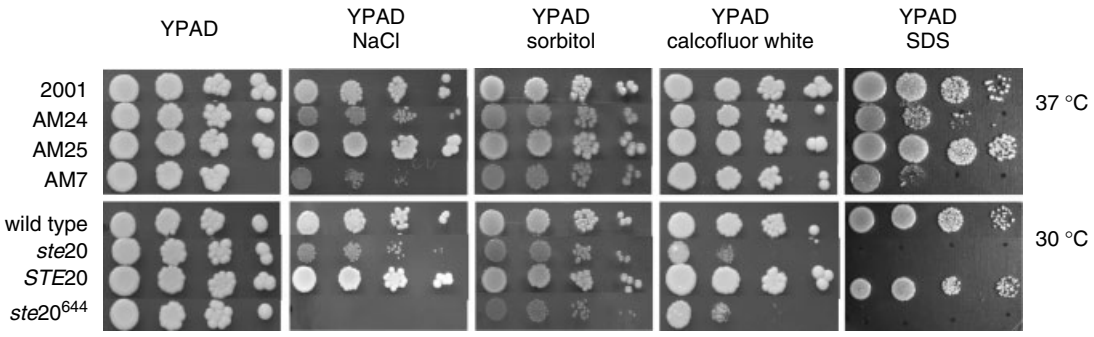

Figure 5. Ste20 plays a redundant role in mediating an appropriate *C. glabrata* hypertonic stress response but is required for maintenance of cell wall integrity. *C. glabrata* wild-type (2001), *ste20* (AM24), reconstituted *STE20* (AM25) and *ste20*^{644} (AM7) strains were cultured on YPAD, YPAD plus 1 M sodium chloride, YPAD plus 1.5 M sorbitol, YPAD plus 1 mg/ml calcofluor white and YPAD plus 0.15% (w/v) SDS at 30 °C or 37 °C for 48 h. Images were captured with a Nikon CoolPix digital camera and imported into and assembled in Microsoft Word

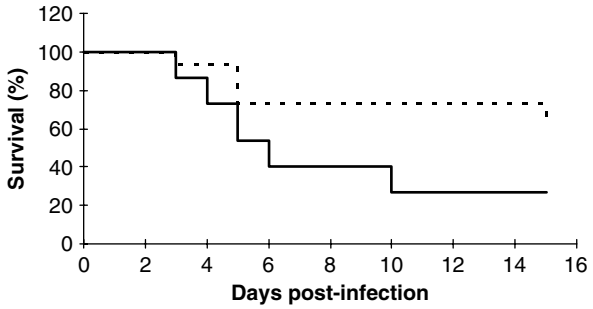

Figure 6. *C. glabrata ste20* mutants are mildly attenuated. Groups of 15 immunosuppressed CD1 mice were inoculated with equivalent doses of either the *C. glabrata STE20* reconstituted strain AM25 (solid line) or the *ste20* null mutant AM24 (hatched line). Mice were sacrificed when the predetermined end-point of 20% weight loss was reached. Kaplan–Meier log rank analysis revealed that the survival curves were significantly different ($p = 0.011$) for the two groups

have demonstrated that *C. glabrata* has a Ste20 homologue that is important in maintaining cell wall integrity, plays a redundant role in adaptation to hypertonic stress and is not required for nitrogen starvation-induced filamentation. Furthermore we show that *C. glabrata ste20* mutants, while still able to cause disease, are attenuated compared to *STE20*-reconstituted cells.

C. glabrata ste20^{644} mutants are unable to grow in the presence of high concentrations of sodium chloride at 30 °C, whereas the null mutant exhibits only a moderate growth defect under these conditions. We speculate that the phenotypic difference observed between mutants could be due to the production of a truncated Ste20 in *C. glabrata* AM7 that retains the N-terminal Cdc42-binding domain that has been shown to be required in the *S. cerevisiae* HOG pathway (Ash *et al.*, 2003; Leberer *et al.*, 1997; Raitt *et al.*, 2000). It is possible that sequestration of Cdc42 to truncated and inactive Ste20 would prevent the activation of a compensatory kinase in *C. glabrata* AM7, but not in the *ste20* null strain AM20, as Cdc42 would not be sequestered. Two Ste20-related protein kinases, Cla4 and Skm1 (Martin *et al.*, 1997) have been found in *S. cerevisiae*, and it is possible that the activation of one of these kinases could partially compensate for the loss of Ste20. A homologue of Cla4 (GAGL–CDS 0666.1) has been annotated in the *C. glabrata* protein sequence release. A possible overlap in functions is suggested, as *S. cerevisiae ste20* and *cla4* mutations are synthetically lethal (Cvrckova *et al.*, 1995). Similarly recent work by (Keniry and Sprague, 2003) demonstrates that Ste20 and Cla4 interact with, and are regulated by, Cdc42. Furthermore, the substitution of a single amino acid in Cla4 conferred upon this protein the ability to perform many apparently Ste20-specific functions. Our data suggest that *C. glabrata* Ste20 plays a role in this species adaptation to hypertonic stress. However, it is clear that Ste20-independent functions also contribute to the hypertonic stress response in *C. glabrata*.

In *S. cerevisiae* the hypertonic stress response pathway can be triggered by three different branches (O'Rourke and Herskowitz, 2002; O'Rourke *et al.*, 2002). The first involves Sln1, Ypd1, Ssk1 and the Ssk2/Ssk22 kinases, while the second involves Sho1, a putative membrane osmosensor that is able to activate Pbs2 via Ste20 and Ste11 (Posas and Saito, 1997). The third involves Msb2 and is partially redundant with the Sho1 branch (O'Rourke and Herskowitz, 2002). The signals are thought to converge at the Pbs2 level, which phosphorylates and activates Hog1. In *S. cerevisiae* the *ste20 ssk2 ssk22* triple mutant cannot grow at high osmolarity. In this strain all the pathways that converge on Pbs2 are interrupted (Posas and Saito, 1997). Previously we have shown that in *C. glabrata* deletion of *STE11* alone was sufficient to prevent growth at high osmolarity (Calcagno *et al.*, unpublished data). Combined with our current observation that *C. glabrata* Ste20 plays a redundant role in the hypertonic stress response we hypothesize that in *C. glabrata*, signals mediating this response converge at or above Ste11, and not at Pbs2 as in *S. cerevisiae*. We are currently attempting to characterize the phosphorylation state of Hog1 in wild-type and *C. glabrata ste20* and *ste11* null mutants in order to determine whether this hypothesis is correct.

S. cerevisiae cell wall integrity is maintained in part by the *STE* vegetative pathway which is thought to sense changes in the integrity of the cell wall in a Och1/Sho1-dependent manner resulting in the transmission of a signal, via Ste20 and Ste11, which activates the transcription factor Ste12 and effects subsequent transcription of genes encoding proteins required for the maintenance of cell wall integrity (Cullen *et al.*, 2000; Lee and Elion, 1999). We have shown previously that *C. glabrata* Ste12 is largely dispensable for maintenance of cell

wall integrity (Calcagno *et al*., 2003). This is not the case for Ste20. *C. glabrata ste*20^{644} and *ste20* strains both exhibit growth defects in the presence of calcofluor white and SDS at 30 °C, and to a lesser extent at 37 °C. These data suggest that the cell integrity pathway in *C. glabrata* is substantially different to that in *S. cerevisiae*.

It is also interesting to note that the *C. glabrata* growth phenotypes are more pronounced at 30 °C than at 37 °C. In addition to the *STE* vegetative pathway cell wall integrity in *S. cerevisiae* is also maintained by the PKC pathway, which orchestrates changes in cellular morphology by controlling the expression of genes encoding enzymes involved in cell wall metabolism (Heinisch *et al*., 1999; Jung and Levin, 1999). The PKC pathway is activated more transiently at 37 °C than at lower temperatures in response to cell wall stress (de Nobel *et al*. 2000; Kamada *et al*., 1995; Wojda *et al*., 2003). It is possible to hypothesize that the activation of a similar PKC pathway in *C. glabrata* at 37 °C would partially compensate for the cell wall defect of *C.glabrata ste20* mutants seen at 30 °C.

We have previously demonstrated that *C. glabrata* cells produce filaments in response to nitrogen starvation (Csank and Haynes, 2000) and that this is absolutely dependent upon Ste12 (Calcagno *et al*., 2003) but largely independent of Ste11 (Calcagno *et al*., unpublished data). *C. glabrata ste20* mutants filament at a similar level to wild-type cells when starved for nitrogen. These data strongly support the view that the nitrogen starvation signal in *C. glabrata* is not transduced via Ste20. Taken together, these data suggest that the filamentation response to nitrogen starvation in *C. glabrata* is mediated by both Ste11-dependent and -independent pathways that converge at or above the level of Ste12. This is markedly different to the situation in both *S. cerevisiae* and *C. albicans*, where many regulators of filamentation are known (Banuett, 1998; Lengeler *et al*., 2000a; Gancedo, 2001). It is possible that the apparent simplicity of the system in *C. glabrata* will make it the most tractable to molecular dissection.

These observations again demonstrate that, while the components of the STE MAP kinase cascade are apparently shared between *S. cerevisiae* and *C. glabrata*, they contribute differently to each yeasts distinct biology. Defining these differences will be crucial in understanding why *C. glabrata* is isolated much more in the context of human disease.

Acknowledgements

We would like to thank Dominique Sanglard for providing the *C. glabrata* genomic library; Bernard Dujon and Christophe Hennequin for allowing us access to pre-publication *C. glabrata* genome sequence information. Financial support was provided by the BBSRC, The Wellcome Trust, Fungal Research Trust, CGD Research Trust and DFG.

References

Ash J, Wu C, Larocque R, *et al*. 2003. Genetic analysis of the interface between Cdc42p and the CRIB domain of Ste20p in *Saccharomyces cerevisiae*. *Genetics* **163**: 2–20.

Banuett F. 1998. Signalling in the yeasts: an informational cascade with links to the filamentous fungi. *Microbiol Mol Biol Rev* **62**: 242–274.

Bodey GP, Mardani M, Hanna HA, *et al*. 2002. The epidemiology of *Candida glabrata* and *Candida albicans* fungemia in immunocompromised patients with cancer. *Am J Med* **112**: 383–385.

Burbelo PD, Drechsel D, Hall A. 1995. A conserved binding motif defines numerous candidate target proteins for both Cdc42 and Rac GTPases. *J Biol Chem* **270**: 29 072–29 074.

Calcagno A, Bignell E, Warn P, *et al*. 2003. *Candida glabrata STE12* is required for wild-type virulence and nitrogen starvation-induced filamentation. *Mol Microbiol* **50**: 1301–1318.

Csank C, Haynes K. 2000. *Candida glabrata* displays pseudohyphal growth. *FEMS Microbiol Lett* **189**: 111–120.

Cullen PJ, Schultz J, Horecka J, *et al*. 2000. Defects in protein. glycosylation cause SHO1-dependent activation of a STE12 signaling pathway in yeast. *Genetics* **155**: 1001–1018.

Cvrckova F, De Virgilio C, Manser E, Pringle JR, Nasmyth K. 1995. Ste20-like protein kinases are required for normal localization of cell growth and for cytokinesis in budding yeast. *Genes Dev* **9**: 1811–1830.

Diekema DJ, Messer SA, Brueggemann SL, *et al*. 2002. Epidemiology of candidemia: 3-year results from the emerging infections an the epidemiology of Iowa organisms study. *J Clin Microbiol* **40**: 1291–1302.

Gancedo JM. 2001. Control of pseudohyphae formation in *Saccharomyces cerevisiae*. *FEMS Microbiol Rev* **25**: 101–123.

Goehring AS, Mitchell DA, Tong AH, *et al*. 2003. Synthetic lethal analysis implicates Ste20p, a p21-activated protein kinase, in polarisome activation. *Mol Biol Cell* **14**: 1501–1516.

Gumbo T, Isada CM, Hall G, Karafa MT, Gordon SM. 1999. *Candida glabrata* Fungemia. Clinical features of 139 patients. *Medicine (Baltimore)* **78**: 222–227.

Hanks SK, Quinn AM. 1991. Protein kinase catalytic domain sequence database: identification of conserved features of primary structure and classification of family members. *Methods Enzymol* **200**: 36–62.

Hanks SK, Quinn AM, Hunter T. 1988. The protein kinase family: conserved features and deduced phylogeny of the catalytic domains. *Science* **241**: 45–52.

Heinisch JJ, Lorberg A, Schmitz HP, Jacoby JJ. 1999. The protein kinase C-mediated MAP kinase pathway involved in the maintenance of cellular integrity in *Saccharomyces cerevisiae*. *Mol Microbiol* **32**: 676–680.

Jung US, Levin DE. 1999. Genome-wide analysis of gene expression regulated by the yeast cell wall integrity signalling pathway. *Mol Microbiol* **34**: 1041–1057.

Kamada Y, Jung US, Piotrowski J, Levin DE. 1995. The protein kinase C-activated MAP kinase pathway of *Saccharomyces cerevisiae* mediates a novel aspect of the heat shock response. *Genes Dev* **9**: 1551–1571.

Keniry ME, Sprague GF Jr. 2003. Identification of p21-activated kinase specificity determinants in budding yeast: a single amino acid substitution imparts Ste20 specificity to Cla4. *Mol Cell Biol* **23**: 1561–1580.

Kitada K, Yamaguchi E, Arisawa M. 1996. Isolation of a *Candida glabrata* centromere and its use in the construction of plasmid vectors. *Gene* **175**: 101–108.

Kohler JR, Fink GR. 1996. *Candida albicans* strains heterozygous and homozygous for mutations in mitogen-activated protein kinase signaling components have defects in hyphal development. *Proc Natl Acad Sci USA* **93**: 13 221–13 228.

Kottom TJ, Kohler JR, Thomas CF Jr, Fink GR, Limper AH. 2003. Lung epithelial cells and extracellular matrix components induce expression of *Pneumocystis carinii* STE20, a gene complementing the mating and pseudohyphal growth defects of STE20 mutant yeast. *Infect Immun* **71**: 6466–6471.

Leberer E, Dignard D, Harcus D, Thomas DY, Whiteway M. 1992. The protein kinase homologue Ste20p is required to link the yeast pheromone response G-protein $\beta\gamma$ subunits to downstream signalling components. *EMBO J* **11**: 4814–4824.

Leberer E, Harcus D, Broadbent ID, *et al*. 1996. Signal transduction through homologs of the Ste20p and Ste7p protein kinases can trigger hyphal formation in the pathogenic fungus *Candida albicans*. *Proc Natl Acad Sci USA* **93**: 13 211–13 222.

Leberer E, Wu C, Leeuw T. 1997. Functional characterization of the Cdc42p binding domain of yeast Ste20p protein kinase. *EMBO J* **16**: 89–97.

Lee BN, Elion EA. 1999. The MAPKKK Ste11 regulates vegetative growth through a kinase cascade of shared signaling components. *Proc Natl Acad Sci USA* **96**: 12 671–12 684.

Leeuw T, Wu C, Schrag JD, *et al*. 1998. Interaction of a G-protein β-subunit with a conserved sequence in Ste20/PAK family protein kinases. *Nature* **391**: 191–195.

Lengeler KB, Davidson RC, D'souza C, *et al*. 2000a. Signal transduction cascades regulating fungal development and virulence. *Microbiol Mol Biol Rev* **64**: 747–785.

Lengeler KB, Wang P, Cox GM, Perfect JR, Heitman J. 2000b. Identification of the MAT**a** mating-type locus of *Cryptococcus neoformans* reveals a serotype A MAT**a** strain thought to have been extinct. *Proc Natl Acad Sci USA* **97**: 14 451–14 460.

Lo HJ, Kohler JR, DiDomenico B, *et al*. 1997. Non-filamentous *C. albicans* mutants are avirulent. *Cell* **90**: 939–949.

Martin H, Mendoza A, Rodriguez-Pachon JM, Molina M, Nombela C. 1997. Characterization of SKM1, a *Saccharomyces cerevisiae* gene encoding a novel Ste20/PAK-like protein kinase. *Mol Microbiol* **23**: 434–444.

Mosch HU, Fink GR. 1997. Dissection of filamentous growth by transposon mutagenesis in *Saccharomyces cerevisiae*. *Genetics* **145**: 676–684.

de Nobel H, Ruiz C, Martin H, *et al*. 2000. Cell wall perturbation in yeast results in dual phosphorylation of the Slt2/Mpk1 MAP kinase and in an Slt2-mediated increase in FKS2–lacZ expression, glucanase resistance and thermotolerance. *Microbiology* **146**: 2122–2132.

O'Rourke SM, Herskowitz I. 1998. The Hog1 MAPK prevents cross-talk between the HOG and pheromone response MAPK pathways in *Saccharomyces cerevisiae*. *Genes Dev* **12**: 2872–2886.

O'Rourke SM, Herskowitz I. 2002. A third osmosensing branch in *Saccharomyces cerevisiae* requires the Msb2 protein and functions in parallel with the Sho1 branch. *Mol Cell Biol* **22**: 4734–4749.

O'Rourke SM, Herskowitz I, O'Shea EK. 2002. Yeast go the whole HOG for the hyperosmotic response. *Trends Genet* **18**: 404–412.

Ottilie S, Miller PJ, Johnson DI, *et al*. 1995. Fission yeast pak1$^+$ encodes a protein kinase that interacts with Cdc42p and is involved in the control of cell polarity and mating. *EMBO J* **14**: 5905–5919.

Pfaller MA, Messer SA, Hollis RJ, *et al*. 1999. Trends in species distribution and susceptibility to fluconazole among blood stream isolates of *Candida* species in the United States. *Diagn Microbiol Infect Dis* **33**: 212–222.

Posas F, Saito H. 1997. Osmotic activation of the HOG MAPK pathway via Ste11p MAPKKK: scaffold role of Pbs2p MAPKK. *Science* **276**: 1701–1705.

Raitt DC, Posas F, Saito H. 2000. Yeast Cdc42 GTPase and Ste20 PAK-like kinase regulate Sho1-dependent activation of the Hog1 MAPK pathway. *EMBO J* **19**: 4624–4631.

Ramer SW, Davis RW. 1993. A dominant truncation allele identifies a gene, STE20, that encodes a putative protein kinase necessary for mating in *Saccharomyces cerevisiae*. *Proc Natl Acad Sci USA* **90**: 454–456.

Wang P, Nichols CB, Lengeler KB, *et al*. 2002. Mating-type-specific and non-specific PAK kinases play shared and divergent roles in *Cryptococcus neoformans*. *Eukaryot Cell* **1**: 252–272.

Weinzierl G, Leveleki L, Hassel A, *et al*. 2002. Regulation of cell separation in the dimorphic fungus *Ustilago maydis*. *Mol Microbiol* **45**: 212–231.

Widmann C, Gibson S, Jarpe MB, Johnson GL. 1999. Mitogen-activated protein kinase: conservation of a three-kinase module from yeast to human. *Physiol Rev* **79**: 141–180.

Wojda I, Alonso-Monge R, Bebelman JP, Mager WH, Siderius M. 2003. Response to high osmotic conditions and elevated temperature in *Saccharomyces cerevisiae* is controlled by intracellular glycerol and involves coordinate activity of MAP kinase pathways. *Microbiology* **149**: 1191–1204.

Wu C, Lee SF, Furmaniak-Kazmierczak E. 1996. Activation of myosin-I by members of the Ste20p protein kinase family. *J Biol Chem* **271**: 31 783–31 790.

Wu C, Lytvyn V, Thomas DY, Leberer E. 1997. The phosphorylation site for Ste20p-like protein kinases is essential for the function of myosin-I in yeast. *J Biol Chem* **272**: 30 623–30 626.

Xu JR. 2000. Map kinases in fungal pathogens. *Fungal Genet Biol* **31**: 131–152.

